GPPS | JOURNAL

JOURNAL OF THE GLOBAL POWER AND PROPULSION SOCIETY
journal.gpps.global

A study of real-gas effect on SCO_2 compressor performance using similitude method

Original article

Article history:
Submission date: 29 June 2022
Acceptance date: 28 July 2022
Publication date: 11 August 2022

This is the updated version of a paper originally presented at the Global Power and Propulsion Virtual Technical Conference, GPPS Xi'an21, April 11–13, 2022.

Check for updates

*Correspondence:
ZZ: zouzhengping@buaa.edu.cn

Peer review:
Single blind

Copyright:
© 2022 Xu and Zou This is an open access article distributed under the Creative Commons Attribution Non Commercial No Derivatives License (CC BY-NC-ND 4.0). Unrestricted use, distribution, and reproduction of the original work are permitted for noncommercial purposes only, provided it is properly cited and its authors credited. No derivative of this work may be distributed.

Keywords:
CO_2 compressor; similitude method; real-gas effect; performance analysis

Citation:
Xu P., Zou Z. (2022). A study of real-gas effect on SCO_2 compressor performance using similitude method. Journal of the Global Power and Propulsion Society. 6: 200–212.
https://doi.org/10.33737/jgpps/152462

Pengcheng Xu[1], Zhengping Zou[2,*]

[1]*National Key Laboratory of Science and Technology on Aero-Engine Aero-thermodynamics, School of Energy & Power Engineering, Beihang University, Beijing 100191, China*
[2]*Research Institute of Aero-engine, Beihang University, Beijing 102206, China*

Abstract

The drastic property changes of supercritical CO_2 (SCO_2) make the performance of SCO_2 compressors different from that of conventional compressors. This study deals with the real-gas effect on the SCO_2 compressor performance by theoretical analysis and numerical validation. A set of similitude parameters are firstly deduced by dimensional analysis. Then keeping these parameters unchanged, the performance variation of a SCO_2 compressor is analyzed when the inlet flow condition changes in a certain temperature and pressure range. Results show that the proposed similitude method could accurately reflect the variation trend of SCO_2 compressor performance under different inflow conditions. The real-gas effect enables the compressor to obtain higher pressure ratio with lower temperature rise. It is recommended that the inlet temperature of SCO_2 compressor should be as close as possible to the critical temperature and the pressure should be about 150 kPa higher than the corresponding pseudo-critical pressure at the same temperature.

Introduction

Nowadays the main use of energy is to convert heat energy into mechanical energy. Even though the heat source may come from nuclear reactor, solar energy, geothermal energy, industrial waste heat, chemical fuel combustion and so on, the conversion system is mainly the closed Brayton cycle with special working fluids. Among the numerous alternative cycling mediums, the supercritical carbon dioxide (SCO_2) is becoming more and more popular due to its high critical temperature which is close to normal temperature and high density which considerably reduced the machine size (Feher, 1968; Dostál et al., 2011; Deng et al., 2017; Yao and Zou, 2020).

It is the compressor that works near the critical point of CO_2 in the closed Brayton cycle system, so the application advantage of CO_2 as the working medium in Brayton cycle system is mainly reflected in CO_2 compressor (Wright et al., 2010; Lettieri et al., 2015; Lee et al., 2016). However, there are few studies which theoretically analyze how the physical properties of CO_2 near the critical point affect the compressor performance. The main difficulty lies in the lack of a set of specifications to restrict other variables so that only the real gas effect is considered. Baltadjiev (Baltadjiev, 2012) avoided the above problem by comparing the one-dimensional nozzle flow of real gas and ideal gas. The results indicated a reduction of 9% in the choke margin compared to its performance at ideal gas conditions. Although it is difficult to directly

OPEN ACCESS

extend the conclusion of one-dimensional nozzle flow to three-dimensional rotating compressor flow, lessons can be drawn from the application of the isentropic pressure exponent n_s (Schultz, 1962) which is of great significance for the flow analysis of real gases. In addition, some researches (Chen et al., 2019a) simply changed the inflow condition of SCO_2 compressors to study the variation of compressor performance. However, due to the inconsistency of the flow field under different conditions, it is hard to ensure that the performance is not affected by other factors.

One possible method is to obtain a series of dimensionless parameters that affect the compressor performance through dimensional analysis (Simon et al., 2017). By remaining these dimensionless parameters unchanged, the performance comparison will be meaningful. This solution, which is called similitude method, is widely adopted in the field of air compressor experiments. In fact, for two similar air compressors, the performance of the two compressors is identical because the physical properties of the working fluids remain unchanged (Dixon and Hall, 2014). In condition that the fluid properties are changed, some researchers have studied the similitude method between different ideal gas compressors. There are several ways to deduced the similarity criteria, including dimensional analysis (Roberts and Sjolander, 2005; Chen et al., 2019b), kinematic similarity derivation (Zou and Ding, 2018) and differential equation method (Zhu et al., 2008). However, when it comes to the near-critical CO_2, the ideal gas assumption can not be satisfied, so the above methods are no longer applicable. Pham (Pham et al., 2016) proposed a set of similitude parameters by introducing the isentropic pressure exponent n_s and compressibility factor Z into the similar parameters of air compressor. However, there may be some deviations due to the lack of strict physical derivation. Jeong (Jeong et al., 2020) used Pham's similitude parameter, but made some numerical correction to the efficiency similitude parameter. Good agreement had been achieved. However, this correction was obtained by trials. Xu (Xu et al., 2021) theoretically deduced a unified performance conversion method for turbomachines working with all kind of fluids, which could be the basis of this work.

In this paper, a set of nondimensional parameters which determine the compressor performance are firstly deduced by dimensional analysis. Since physical properties of CO_2 vary with different compressor inlet conditions, it is hardly possible to keep all the physical property parameters unchanged. Thus, this paper proposed a set of new similitude parameters which may ensure approximate similarity between real gas compressors by combining the physical property parameters and the deduced nondimensional parameters. Then keeping these similitude parameters unchanged, the variation of a SCO_2 compressor performance is studied when its inlet condition changes along an isotherm line and an isobar line near the critical point. Numerical simulations are also adopted for validation. Finally, using this similitude method, the performance distribution of a SCO_2 compressor in a certain range of inlet pressure and temperature is given. The influence of the real-gas effect on the compressor performance is summarized, and some suggestions on the designed inlet flow condition of the SCO_2 compressor are given.

Methodology

Physical properties of carbon dioxide

The specific heat Cp, compressibility factor Z and enthalpy H of CO_2 in a certain range are displayed in Figure 1. This range ($T = 310$ K $- 360$ K, $P = 7.4$ MPa $- 8.2$ MPa) is selected because the incoming flow for most SCO_2 compressors lies in it. A sharp tip of the Cp surface could be found near the critical point, indicating that in SCO_2 compressors the specific heat Cp of the working fluid could no longer be regarded as constant. It can also be found that near the critical temperature, the compressibility factor Z deviates a lot from 1, which indicates that the ideal gas hypothesis is no longer applicable. In addition, the enthalpy of CO_2 is not only related to temperature, but also affected by the pressure. Obviously there is a coupling effect between pressure rise and enthalpy increase. Overall, the real gas CO_2 behaves totally differently from the ideal gas near the critical point so it is necessary to study the real-gas effect of CO_2 on the performance of compressors.

Dimensional analysis

The performance of a compressor can be expressed in terms of the control variables, geometric variables, and fluid properties. The geometric variables are characterized by the impeller diameter D, while others are gathered as $L = (l_1, l_2, l_3, \ldots)$. The control variables include the inlet total temperature T_{01}, the inlet total pressure P_{01}, the mass flow rate $\dot{m}$ and the rotational speed n. The fluid properties consist of the gas constant R_g, the specific heat ratio γ and kinematic viscosity υ. The compressor performance is reflected in terms of enthalpy rise ΔH,

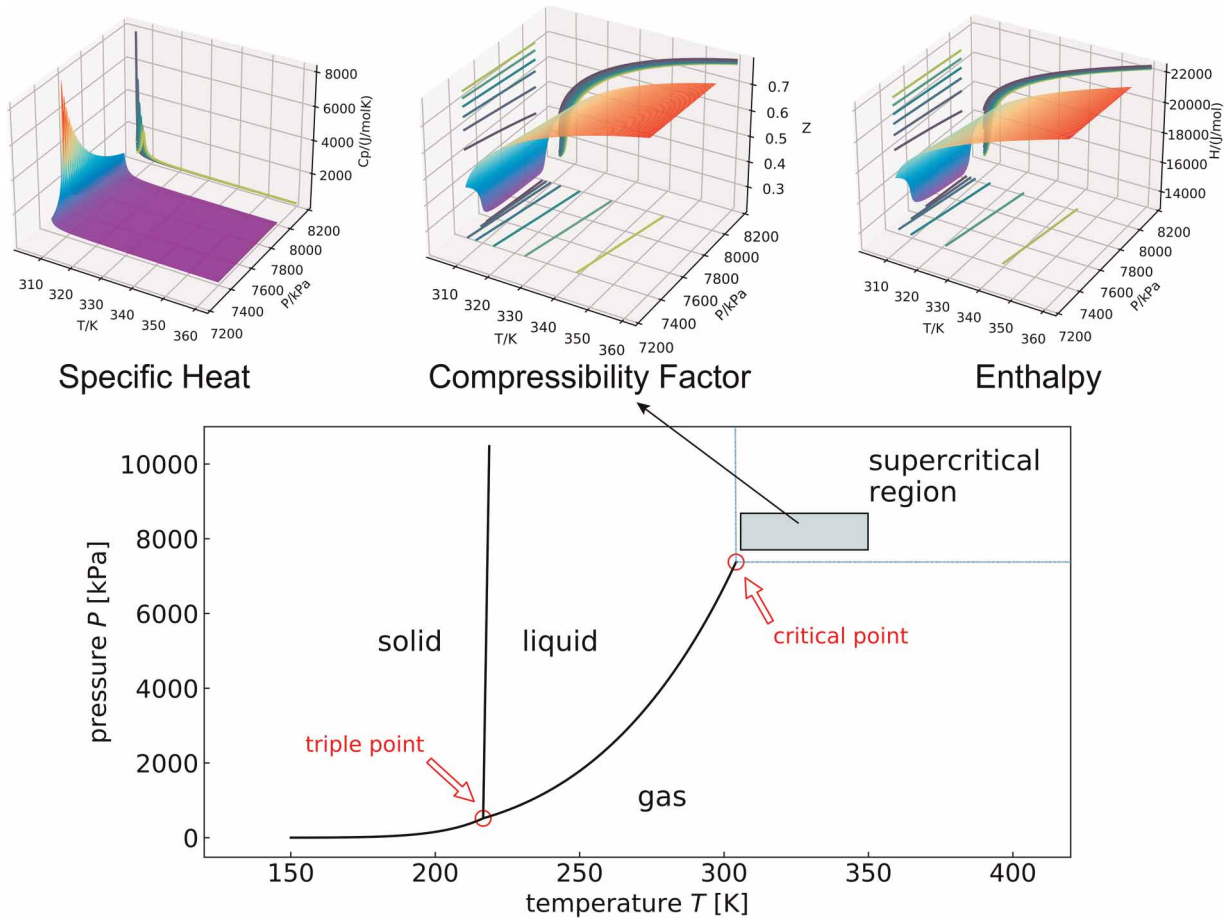

Figure 1. Physical properties of carbon dioxide.

pressure ratio π and efficiency η. Since there is a certain conversion relationship between these three performance parameters, only the enthalpy rise ΔH and efficiency η are selected to represent the compressor performance.

Due to the strong nonlinear characteristics of the physical properties near the critical point for CO_2, the state equation of ideal gas is no longer applicable. In addition, the specific heat ratio cannot reflect the isentropic change process of working fluid alone. Hence, the compressibility factor Z and the isentropic pressure exponent n_s are introduced to describe real gas properties. They are defined as follows:

$$Z = \frac{pV}{R_g T} \tag{1}$$

$$n_s = \frac{\gamma}{\alpha_T P} = -\gamma \frac{V}{P}\left(\frac{\partial P}{\partial V}\right)_T \tag{2}$$

where α_T is the isothermal compressibility and is defined as $-(\partial V/\partial P)_T/V$. For ideal gases, $\alpha_T = 1/P$, so $n_s = \gamma$.

Now it is convenient to write the two functional relationships as

$$\Delta H = f(\dot{m}, n, T_{01}, P_{01}, R_g, Z_0, n_s, \upsilon, D, L) \tag{3}$$

$$\eta = g(\dot{m}, n, T_{01}, P_{01}, R_g, Z_0, n_s, \upsilon, D, L) \tag{4}$$

Choosing the parameters (T_{01}, P_{01}, R_g, D) as dimensions, these two relationships can be reduced to the following forms based on Buckingham's π-theory (Buckingham, 1914):

$$\frac{\Delta H}{R_g T_{01}} = f\left(\frac{\dot{m}\sqrt{R_g T_{01}}}{P_{01} D^2}, \frac{nD}{\sqrt{R_g T_{01}}}, Z_0, n_s, \frac{nD^2}{\upsilon}, \frac{L}{D}\right) \tag{5}$$

$$\eta = g\left(\frac{\dot{m}\sqrt{R_g T_{01}}}{P_{01} D^2}, \frac{nD}{\sqrt{R_g T_{01}}}, Z_0, n_s, \frac{nD^2}{\upsilon}, \frac{L}{D}\right) \tag{6}$$

where $\left(\dot{m}\sqrt{R_g T_{01}}\right)/(P_{01}D^2)$ is nondimensional mass flow, $(nD)/\sqrt{R_g T_{01}}$ is nondimensional blade tip speed, Z_0 and n_s are fluid properties which are already nondimensional, $(nD^2)/\upsilon$ is the Reynolds number and L/D is nondimensional shape parameter.

Obviously, full similarity can only be achieved when the above six nondimensional parameters are all identical. However, no matter for the similarity between the real gas and the ideal gas compressor, or for the similarity between the real gas compressors with different inlet conditions, it is impossible to ensure that all physical parameters are equal. Therefore, refer to Chen's work (Chen et al., 2019b), we derived a set of new similitude parameters to achieve approximate similarity by combining those nondimensional parameters and fluid property parameters. The forms are as follows:

$$\left\langle \frac{\Delta H}{R_g T_{01}}, Z_0, n_s \right\rangle = f\left(\left\langle \frac{\dot{m}\sqrt{R_g T_{01}}}{P_{01} D^2}, Z_0, n_s \right\rangle, \left\langle \frac{nD}{\sqrt{R_g T_{01}}}, Z_0, n_s \right\rangle, \frac{nD^2}{\upsilon}\right) \tag{7}$$

$$\left\langle \eta, Z_0, n_s \right\rangle = g\left(\left\langle \frac{\dot{m}\sqrt{R_g T_{01}}}{P_{01} D^2}, Z_0, n_s \right\rangle, \left\langle \frac{nD}{\sqrt{R_g T_{01}}}, Z_0, n_s \right\rangle, \frac{nD^2}{\upsilon}\right) \tag{8}$$

In the Equations 7 and 8, the bracket represents a new parameter composed of its internal parameters. Its specific expression will be derived in the next section.

Similitude parameters

In this section, the specific expressions for the mass flow similitude parameter, the compressibility similitude parameter, the pressure ratio similitude parameter and the efficiency similitude parameter are deduced based on some similarity assumptions.

$\langle\left(\dot{m}\sqrt{R_g T_{01}}\right)/(P_{01}D^2), Z_0, n_s\rangle$ is the similitude parameter for the mass flow. In this paper, it is assumed that similar compressors shares similar shapes of characteristic curves, and the relative positions of two similar points on their respective characteristic curves are the same. Consequently, the similitude parameter of mass flow, which means the swallowing capacity of the compressor, can be defined as

$$\Pi_{\dot{m}} = \left\langle \frac{\dot{m}\sqrt{R_g T_{01}}}{P_{01} D^2}, Z_0, n_s \right\rangle = \frac{\dot{m}}{\dot{m}_{cr}} \tag{9}$$

According to the real gas thermodynamics, the mass flow and critical mass flow are

$$\dot{m} = \frac{P_0}{\sqrt{Z_0 R_g T_0}} D^2 \mathrm{Ma}\sqrt{n_s}\left(1 + \frac{n_s - 1}{2}\mathrm{Ma}^2\right)^{-((n_s+1)/(2(n_s-1)))} \tag{10}$$

$$\dot{m}_{cr} = \frac{P_0}{\sqrt{Z_0 R_g T_0}} D^2 \sqrt{n_s}\left(1 + \frac{n_s - 1}{2}\right)^{-((n_s+1)/(2(n_s-1)))} \tag{11}$$

Therefore, the similitude parameter for the mass flow is

$$\Pi_{\dot{m}} = \frac{\dot{m}\sqrt{R_g T_{01}}/P_{01} D^2}{\sqrt{(n_s/Z_0)((2/(n_s+1)))^{((n_s+1)/(n_s-1))}}} \tag{12}$$

$\langle (nD)/\sqrt{R_g T_{01}}, Z_0, n_s \rangle$ is the similitude parameter for the blade tip speed, which should be nondimensionalized by the sound speed. According to the real-gas thermodynamics, the sound speed is $a = \sqrt{n_s Z_0 R_g T_0}$. Then the similitude parameter for the blade tip speed could be written as:

$$\Pi_U = \frac{nD}{\sqrt{n_s Z_0 R_g T_0}} \tag{13}$$

$\langle \eta, Z_0, n_s \rangle$ is the similitude parameter for the isentropic efficiency. The author's previous work (Xu et al., 2021) has theoretically derivated the similitude parameter for efficiency. It it proved that the polytropic efficiency η_p is much more suitable for performance conversion between similar compressors working with different gases. This is because the polytropic efficiency η_p is independent of the pressure ratio, enthalpy increase, inlet flow conditions, and fluid physical properties. The influences of all these factors are actually manifested in the conversion process from η_p to η_s. So here we choose the polytropic efficiency η_p as the similitude parameter, which is

$$\Pi_\eta = \eta_p \tag{14}$$

Since it is much more popular to use isentropic efficiency η_s rather than polytropic efficiency η_p in engineering, conversion between these two kinds of efficiency is necessary. Detailed conversion method has been presented in the author's previous work (Xu et al., 2021).

$\langle \Delta H/(R_g T_{01}), Z_0, n_s \rangle$ is the similitude parameter for the enthalpy rise, it can be deduced that

$$\frac{\Delta H/(R_g T_0)}{\Pi_U^2} = n_s Z_0 \frac{u \Delta c_u}{u^2} \tag{15}$$

For similar velocity triangles, there is

$$\Pi_{\Delta H} = \frac{\Delta H}{n_s Z_0 R_g T_0} \tag{16}$$

Above all, the final similitude parameters are as follows

$$\frac{\Delta H}{n_s Z_0 R_g T_0} = f\left(\frac{\dot{m}\sqrt{R_g T_{01}}/P_{01} D^2}{\sqrt{n_s/Z_0((2/n_s+1))^{((n_s+1)/(n_s-1))}}}, \frac{nD}{\sqrt{n_s Z_0 R_g T_0}}, \frac{nD^2}{\upsilon} \right) \tag{17}$$

$$\eta_p = g\left(\frac{\dot{m}\sqrt{R_g T_{01}}/P_{01} D^2}{\sqrt{n_s/Z_0((2/(n_s+1)))^{((n_s+1)/(n_s-1))}}}, \frac{nD}{\sqrt{n_s Z_0 R_g T_0}}, \frac{nD^2}{\upsilon} \right) \tag{18}$$

Approximate similarity

While the fluid properties are not completely identical, only approximate similarity can be achieved using the above similarity criterion. Thus, it is necessary to evaluate the degree of similarity. The similarity of compressor can be evaluated from two aspects, namely, kinematics similarity and dynamic similarity. The kinematics similarity means that the inlet and outlet velocity triangles of the compressor are proportional respectively, which can be quantified by c_{m1}/u and c_{m1}/c_{m2}. The dynamic similarity means that the magnitude and direction of the same force on the corresponding point in the flow field are proportional, which specifically include the axial Mach number Ma_{1a}, the rotational Mach number Mu and the Reynold number Re. Since Mu and Re are the similitude parameters, only c_{m1}/u, c_{m1}/c_{m2} and Ma_{1a} are considered.

For two compressors with the identical geometry but different working media, assuming that the working fluids are A and B respectively, the following two equations can be derived when $\Pi_{\dot{m}}$, Π_U and Re are identical.

$$\frac{(c_{m1}/u)_B}{(c_{m1}/u)_A} = \frac{(1+((n_{sB}-1)/2)\mathrm{Ma}_{1B}^2)^{(1/(n_{sB}-1))}}{(1+((n_{sA}-1)/2)\mathrm{Ma}_{1A}^2)^{(1/(n_{sA}-1))}} \frac{\sqrt{((2/(n_{sB}+1)))^{((n_{sB}+1)/(n_{sB}-1))}}}{\sqrt{((2/(n_{sA}+1)))^{((n_{sA}+1)/(n_{sA}-1))}}} \tag{19}$$

$$(\mathrm{Ma}_{1a})_A\left[\frac{2}{n_{sA}+1}\left(1+\frac{n_{sA}-1}{2}(Ma_{1a}^2)_A\right)\right]^{-((n_{sA}+1)/2(n_{sA}-1))} = (Ma_{1a})_B\left[\frac{2}{n_{sB}+1}\left(1+\frac{n_{sB}-1}{2}(Ma_{1a}^2)_B\right)\right]^{-((n_{sB}+1)/(2(n_{sB}-1)))} \tag{20}$$

Setting n_{sA} to a constant value of 1.29, Figure 2 shows the variation of $(c_1/u)_B/(c_1/u)_A$ with axial Mach number Ma_{1a} when n_{sB} changes from 1.3 to 1.9. It can be seen that greater difference in n_s will lead to larger deviation in kinematics similarity. If the n_s difference is small, the variation of the incoming Mach number Ma_{1a} has little effect on the similarity of the compressor. However, when the n_s difference is large, the degree of kinematics similarity decreases with a growing Ma_{1a} while the degree of dynamic similarity increases. In general, for different inlet conditions, if the isentropic pressure exponent n_s changes a lot, there will be assignable errors exist no matter for the kinematics similarity or for the dynamic similarity. Therefore, further validation is necessary for the similitude method.

Results and discussion

Validation of the similitude method

A typical SCO_2 centrifugal compressor with near-critical designed inlet condition is selected for further validation. Detailed dimensions and the operation conditions of this compressor at the design point are listed in Table 1. With identical geometry, numerical simulations are performed with ideal CO_2 gas and real CO_2 gas. The commercial software ANSYS CFX 19.0 is used to solve steady viscous Reynolds Averaged Navier-Stokes equations with a time marching finite volume method. The spatial discretization adopts a second-order upwind scheme and the temporal discretization adopts a second-order backward Euler scheme. The shear stress transport (SST) turbulence model is used. In the numerical calculation, only one passage is simulated so that surfaces at circumferential side are set as periodic boundary conditions. Total temperature, total pressure, and inflow angle are used as the inlet boundary conditions, and static pressure is used as the outlet boundary condition. All the wall faces are set as adiabatic with no slip.

Fully structured grids were generated using Autogrid5. An H-type grid topology is used in the mainstream passage, and an O-type topology is adopted near the blade wall and inside the tip gap. The mesh around the leading edge and trailing edge is locally refined. Mesh dependency test was done by computing the total to total isentropic efficiency and total to total pressure ratio changes for different grid sizes. It was found that grids with

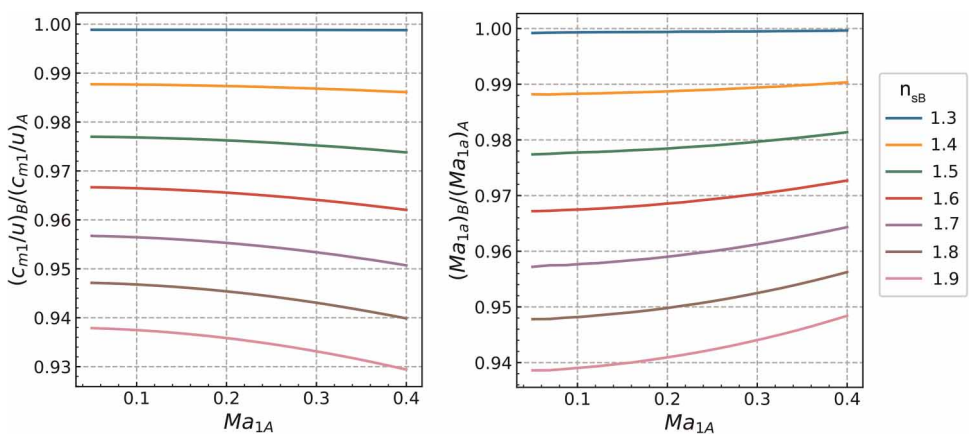

Figure 2. Evaluation of approximate similarity for different working fluid B when $n_{sA} = 1.29$.

Table 1. Informations of the simulated compressor.

T_{01}	P_{01}	r_{1h}	r_{1s}	r_2	β_{2b}
320 K	7,600 kPa	30 mm	68 mm	152 mm	−33°

around 1.1 million nodes are dense enough to provide grid-independent results. Sufficiently fine cells near the walls were generated to ensure the values of y^+ close to unity. Figure 3 demonstrates the studied centrifugal compressor and the structured grid.

The CFX bulit-in ideal gas model for CO_2 is selected for the ideal CO_2 compressor simulation. As for the real gas CO_2 compressor, an external real gas properties (RGP) look-up table is used to define the properties of CO_2 such as enthalpy, entropy, pressure, temperature, density, sound speed, specific heat in constant pressure and viscosity. The abovementioned properties are taken from the widely used NIST REFPROP 9.0 database (Lemmon et al., 2002). RGP table resolution is gradually increased when getting closer to the critical point and the minimum interval of the pressure and the temperature are 10 kPa and 0.1 K respectively. The table covers sufficient wide ranges of temperature and pressure to prevent clipping or extrapolating of the properties. To validate the accuracy of the fluid thermodynamic property interpolation, the simulated properties at a point near the critical point and a point away from the critical point are compared with the REFPROP database. Results are showed in Table 2 and it is found that the error is less than 0.2%, indicating that the look-up table is suitable for CFD simulations.

A real gas SCO_2 compressor and an ideal gas CO_2 compressor with identical ($\Pi_{\dot{m}}$, Π_U, Re) are simulated. The characteristic curves of the ideal gas CO_2 compressor can be easily transformed to the similar real gas SCO_2 compressor characteristic curves. Results are displayed in Figure 4. The simulated real gas SCO_2 compressor characteristic curves are presented for comparison. The original ideal gas CO_2 compressor characteristic curves are also showed. It can be seen that without transformation, performance maps for ideal gas and real gas are totally different. But if the similitude method is imposed, fair good agreement can be achieved for the pressure ratio. As for the efficiency curves, the proposed similitude method is able to predict the efficiency with errors less than 1% except for the choking region. The maximum error which occurs at the choke point is nearly 2%.

The performance parameters at design point are listed in Table 3 for each compressor. It can be observed that the relative deviation of performance prediction via the similitude method is no more than 1%, which demonstrates the high accuracy of the similitude method at the design point.

Velocity triangles at 10%, 50%, 90% span are given in Figure 5, in which the red arrows refer to real gas and the blue arrows refer to ideal gas. It can be observed that the velocity triangles of the ideal gas compressor are

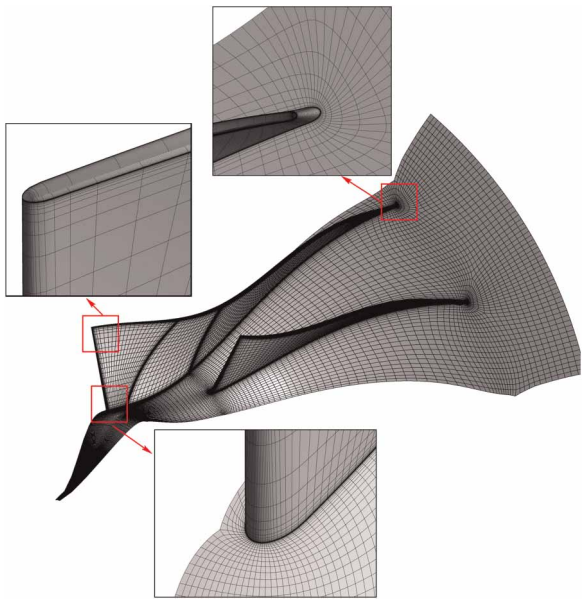

Figure 3. Sketch of computational mesh.

Table 2. Validation of the RGP look-up table.

	Point1			Point2		
	T = 307.93 K, P = 6.48 MPa			T = 368.85 K, P = 13.62 MPa		
	RGP	NIST	error	RGP	NIST	error
$\rho/[\mathrm{kg/m^3}]$	184.69	184.91	0.119%	302.00	302.07	0.023%
$Cp/[\mathrm{J/(kg \cdot K)}]$	2,556.33	2,561.40	0.198%	2,055.89	2,056.31	0.021%

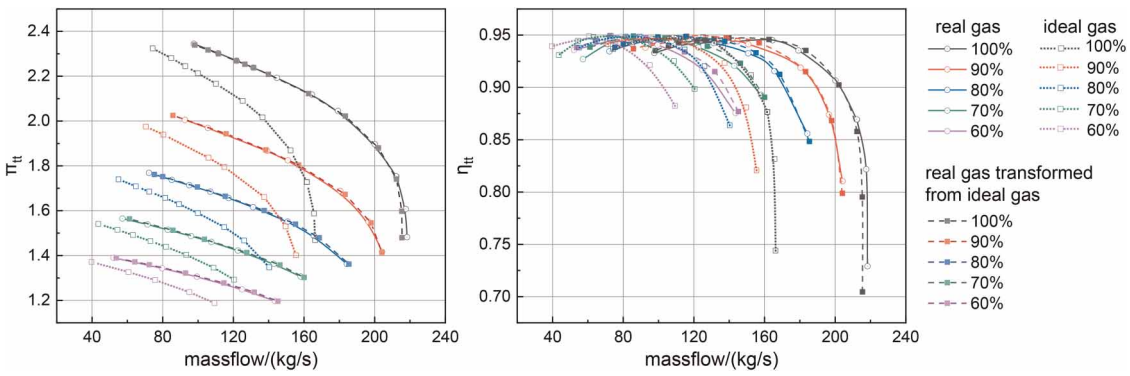

Figure 4. Comparison of the characteristic curves.

Table 3. Comparison of the performance at design point.

	n/rpm	$\dot{m}/(\mathrm{kg/s})$	π_{tt}	$\eta_{s,tt}$
Real gas CO_2	14,000	131.51	2.237	0.9472
Ideal gas CO_2	17,522	99.95	2.213	0.9463
Transformed	14,000	131.27	2.238	0.9464
Error	–	–	0.045%	0.084%

highly similar to those of the real gas compressor at identical locations except for the shroud region. Due to the existence of the low speed region near the impeller shroud, the mass flow through this region accounts for only a small proportion, so the deviation of the velocity triangle in this region has little effect on the prediction of the pressure ratio. Generally speaking, the assumption that the velocity triangle is similar in deriving the performance similitude parameters is reasonable.

Comparison of relative Mach number contours at inlet and outlet is presented in Figure 6. It is showed that the distribution of relative Mach number at these planes in the ideal gas compressor is in good accordance with that in real gas compressor. There are only some differences in numerical values, which further proves that the proposed similitude method can guarantee the dynamic approximate similarity.

Real-gas effect on the SCO_2 compressor performance

In this section, the ideal gas CO_2 compressor above is transformed to real gas SCO_2 compressor with different inlet conditions, and the real-gas effect of CO_2 on compressor performance is studied on that basis.

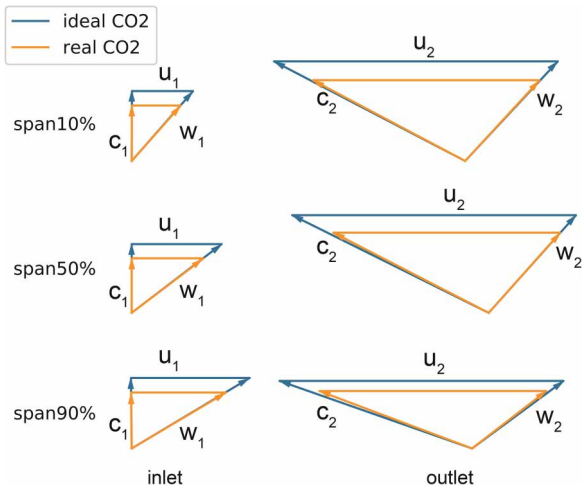

Figure 5. Comparison of the velocity triangles at design point.

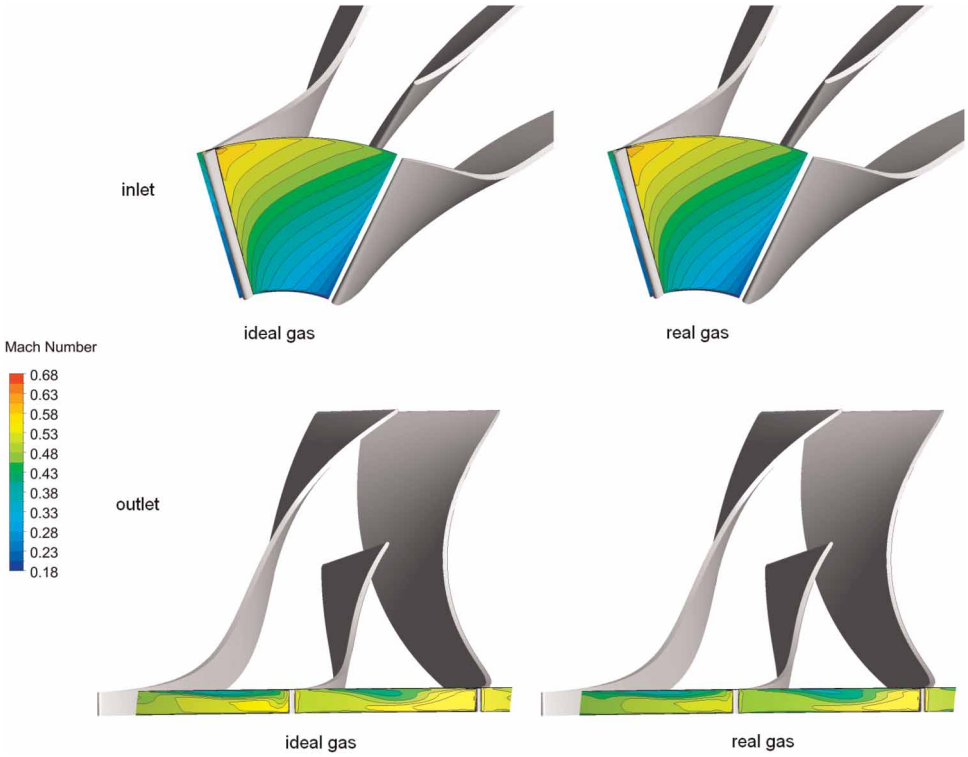

Figure 6. Comparison of the relative Mach number at design point.

Figure 7 shows the variation of compressor performance with the inlet total temperature along the isobar line $P_{01} = 7.6$ MPa. The curve represents the transformed data from the ideal gas CO_2 compressor, and the scatter represents the CFD results under the similar conditions. It can be seen that the similitude method can accurately predict the change of the compressor pressure ratio and temperature ratio. The efficiency may be a little different but the change trend is correctly predicted, which is enough for the discussion. Along the isobar line, with the increase of inlet temperature, the compressibility factor Z_0 gradually increases, while the isentropic component n_s gradually decreases, which means that the real-gas effect is weakened gradually. Correspondingly, compressor pressure ratio gradually decreases, the efficiency gradually decreases, while the temperature ratio gradually increase. That is to say, along an isobar line, if the inlet condition approaches the critical point from the gas side, the real-gas effect becomes stronger, and higher the pressure ratio of the compressor can be obtained through lower temperature rise, with a little efficiency increment.

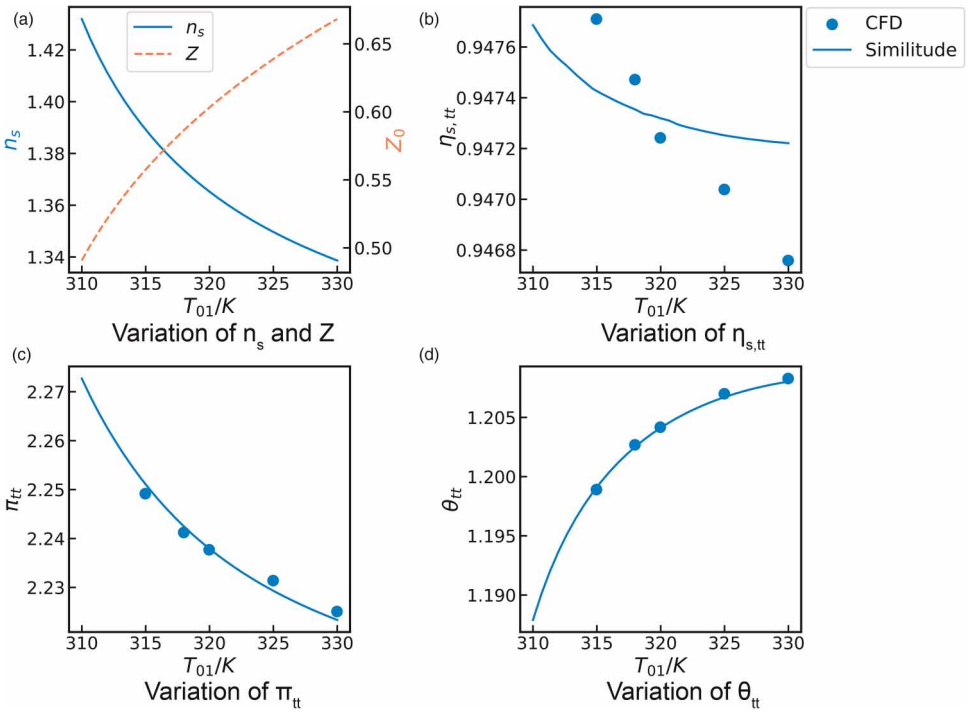

Figure 7. Performance variation with the inlet total temperature at the isobar line P_{01} = 7.6 MPa.

Figure 8 shows the variation of compressor performance with the inlet total pressure along the isotherm line $T_{01} = 320$ K. The curve represents the transformed data from the ideal gas CO_2 compressor, and the scatter represents the CFD results under the similar conditions. It can be seen that along the isotherm line, with the increase of inlet pressure, the compressibility factor Z_0 gradually decreases, while the isentropic component n_s gradually increases, which means that the real-gas effect is enhanced gradually. Correspondingly, compressor pressure ratio and efficiency gradually increases, while the temperature ratio gradually decrease. This lead to the same conclusion about the advantage of real-gas effect as the previous paragraph.

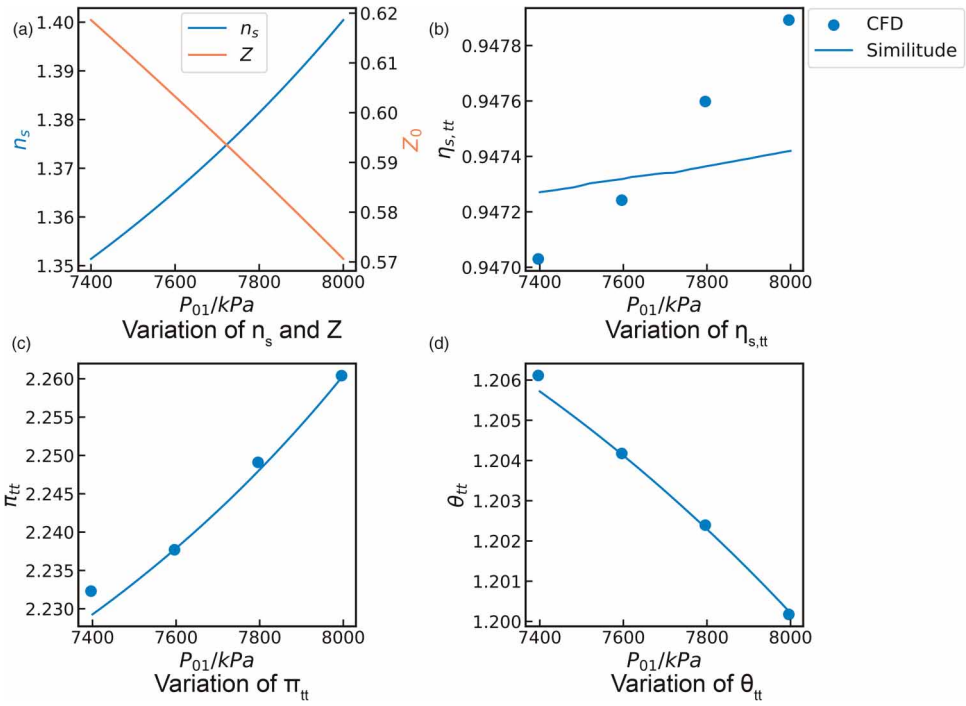

Figure 8. Performance variation with the inlet total pressure at the isotherm line T_{01} = 320 K.

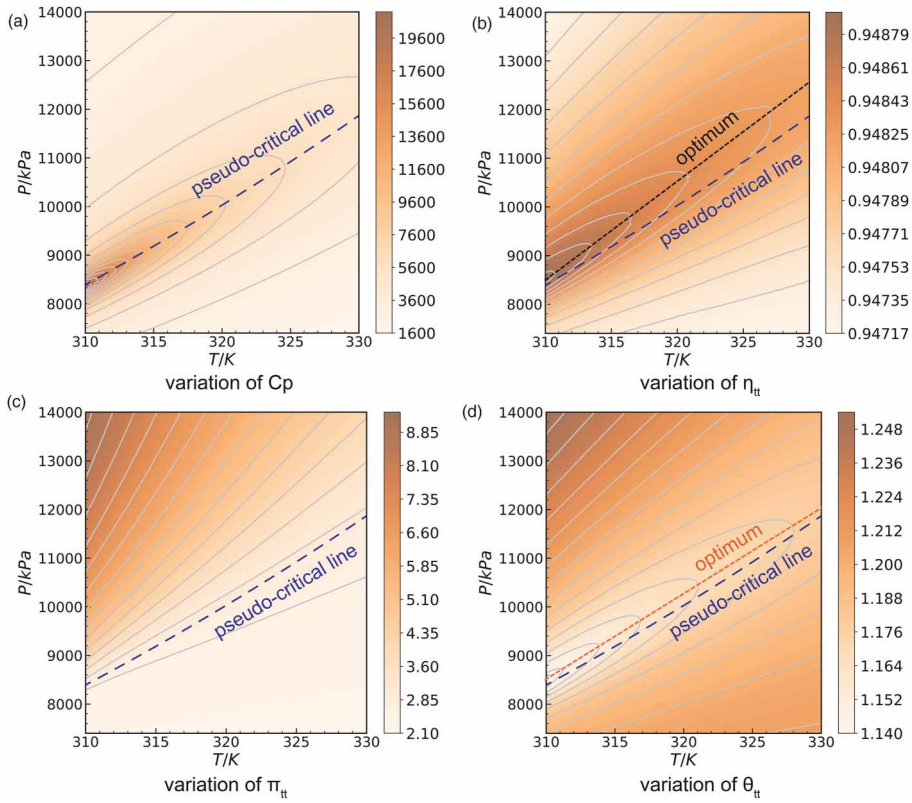

Figure 9. Performance variation with the couple effect of inlet total temperature and pressure.

In the same way, the contour of compressor performance parameters in a larger temperature and pressure range can be drawn, as shown in Figure 9. The pseudo-critical line is also drawn as a reference. The pseudo-critical line in this paper is defined as the path where the gradient of Cp is minimum in the $T-P$ map. It can be described by the following equation:

$$\ln\left(\frac{P}{P_{cr}}\right) = a + b\frac{T_{cr}}{T} + c\ln\left(\frac{T}{T_{cr}}\right) \tag{21}$$

where $a = 4.29$, $b = -4.27$, $c = 1.48$.

It can be seen that for similar SCO_2 compressors, with the increase of inlet pressure or decrease of inlet temperature, the compressor's pressure ratio gradually increases. When the inlet condition moves across the pseudo-critical line, the change rate of pressure ratio increases sharply. As for the temperature ratio and the efficiency, there is an optimal T-P relationship which makes the temperature ratio lowest and the efficiency highest. The optimal pressure is about 150 kPa higher than the pseudo-critical pressure near the critical point. In sum, the real-gas effect enables the compressor to obtain higher pressure ratio with a lower temperature rise and a bit higher efficiency, which is the advantage of the SCO_2 as the working fluid. This advantage will be enhanced when the inlet temperature gets close to the critical temperature and when the inlet pressure gets close to the optimal pressure. Therefore, it is recommended that the designed inlet condition of SCO_2 compressors should be taken near the critical temperature and about 150 kPa higher than the pseudo-critical line.

Conclusion

Several conclusions are drawn as follow:

- Based on the dimensional analysis method and the real gas thermodynamics, a set of approximate similarity criteria for real gases is established, which consists of similitude parameters for mass flow $((\dot{m}\sqrt{R_g T_{01}}/P_{01}D^2)/\sqrt{(n_s/Z_0)((2/(n_s+1)))^{((n_s+1)/(n_s-1))}})$, for compressibility $nD/\sqrt{n_s Z_0 R_g T_0}$, for viscosity nD^2/υ, for enthalpy rise $\Delta H/(n_s Z_0 R_g T_0)$ and for efficiency η_p.

- When the similitude parameters remain unchanged, the pressure ratio of SCO_2 compressor decreases with the increase of inlet temperature and increases with the increase of inlet pressure. As for the temperature ratio and the efficiency, at a specific inlet temperature, there is always an optimal inlet pressure which can minimize the compressor temperature ratio and maximize the efficiency. The optimal pressure is about 150 kPa higher than the pseudo-critical pressure.
- The real-gas effect enables the SCO_2 compressor to obtain higher pressure ratio with lower temperature rise, which is the advantage of SCO_2 as a working fluid. It is recommended that the inlet temperature of SCO_2 compressor should be as close to the critical temperature as possible, and inlet pressure should be about 150 kPa higher than the pseudo-critical pressure.

Nomenclature

Latin letters

$\dot{m}$ Mass flow (kg/s)
c Absolute velocity (m/s)
C_p Specific heat at constant pressure [J/(kg·K)]
D Impeller diameter (m)
H Enthalpy (J/kg)
Ma Mach number (–)
Mu Impeller tip-speed Mach number (–)
n Rotational speed (rpm)
n_s Isentropic pressure exponent (–)
P Pressure (kPa)
r Radius (mm)
R_g Gas constant (J/(kg·K))
T Temperature (K)
u Impeller blade tip speed (m/s)
Z Compressibility factor (–)

Greek letters

α_T Isothermal compressibility (–)
η_p Polytropic efficiency (–)
η_s Isentropic efficiency (–)
γ Specific heat ratio (–)
Π Similitude parameter (–)
π Pressure ratio (–)
ρ Density (kg/m^3)
θ Temperature ratio (–)
υ Kinematic viscosity (m^2/s)

Subscripts

0 Total thermodynamic condition
1 Impeller inlet
cr Critical
tt Total to total

Funding sources

This research was supported by the DITDP (No. 601B013) and the Academic Excellence Foundation of BUAA for Ph.D. students, which are all gratefully acknowledged.

Competing interests

Xu Pengcheng declares that he has no conflict of interest. Zou Zhengping declares that he has no conflict of interest.

References

Baltadjiev N. D. (2012). An Investigation of real gas effects in supercritical CO_2 compressors, Master of Science Thesis, Massachusetts Institute of Technology.

Buckingham E. (1914). On physically similar systems; illustrations of the use of dimensional equations. Physical review. 4 (4): 345. Publisher: APS. https://doi.org/10.1103/PhysRev.4.345

Chen H., Zhuge W., Zhang Y., and Liu H. (2019a). Effect of Compressor Inlet Condition on Supercritical Carbon Dioxide Compressor Performance, American Society of Mechanical Engineers Digital Collection.

Chen Y., Zou Z., and Fu C. (2019b). A study on the similarity method for helium compressors. *Aerospace Science and Technology*. 90: 115–126. https://doi.org/10.1016/j.ast.2019.04.026

Deng Q. H., Wang D., Zhao H., Huang W. T., Shao S., and Feng Z. P. (2017). Study on performances of supercritical CO_2 recompression Brayton cycles with multi-objective optimization. *Applied Thermal Engineering*. 114: 1335–1342. https://doi.org/10.1016/j.applthermaleng.2016.11.055

Dixon S. L. and Hall C. (2014). *Fluid mechanics and thermodynamics of turbomachinery*, 7th edn. Oxford, UK: Butterworth-Heinemann of Elsevier Inc.

Dostál V., Driscoll M., and Hejzlar P. (2011). A Super Critical Carbon Dioxide Cycle for Next Generation Nuclear Reactors, PhD thesis.

Feher E. G. (1968). The supercritical thermodynamic power cycle. *Energy Conversion*. 8 (2): 85–90. https://doi.org/10.1016/0013-7480(68)90105-8

Jeong Y., Son S., Cho S. K., Baik S., and Lee J. I. (2020). Evaluation of supercritical CO_2 compressor off-design performance prediction methods. *Energy*. 213: 119071. https://doi.org/10.1016/j.energy.2020.119071

Lee J., Baik S., Cho S. K., Cha J. E., and Lee J. I. (2016). Issues in performance measurement of CO_2 compressor near the critical point. *Applied Thermal Engineering*. 94: 111–121. https://doi.org/10.1016/j.applthermaleng.2015.10.063

Lemmon E. W., Huber M. L., and McLinden M. O. (2002). NIST reference fluid thermodynamic and transport properties—REFPROP, *NIST standard reference database* **23**, v7.

Lettieri C., Yang D., and Spakovszky Z. (2015). An investigation of condensation effects in supercritical carbon dioxide compressors. *Journal of Engineering for Gas Turbines and Power*. 137 (8): 082602. https://doi.org/10.1115/1.4029577

Pham H. S., Alpy N., Ferrasse J. H., Boutin O., Tothill M., et al. (2016). An approach for establishing the performance maps of the sc-CO2 compressor: development and qualification by means of CFD simulations. *International Journal of Heat and Fluid Flow*. 61: 379–394. https://doi.org/10.1016/j.ijheatfluidflow.2016.05.017

Roberts S. K. and Sjolander S. A. (2005). Effect of the specific heat ratio on the aerodynamic performance of turbomachinery. *Journal of Engineering for Gas Turbines and Power*. 127 (4): 773–780. https://doi.org/10.1115/1.1995767

Schultz J. M. (1962). The polytropic analysis of centrifugal compressors. *Journal of Engineering for Power*. 84 (1): 69–82. https://doi.org/10.1115/1.3673381

Simon V., Weigand B., and Gomaa H. (2017). Dimensional analysis for engineers. Berlin, Germany: Springer.

Wright S. A., Radel R. F., Vernon M. E., Pickard P. S., and Rochau G. E. (2010). Operation and analysis of a supercritical CO_2 Brayton cycle., Technical Report SAND2010-0171, 984129.

Xu P., Zou Z., and Yao L. (2021). A unified performance conversion method for similar compressors working with different gases based on polytropic analysis and deep-learning improvement. *Energy Conversion and Management*. 247: 114747. https://doi.org/10.1016/j.enconman.2021.114747

Yao L. and Zou Z. (2020). A one-dimensional design methodology for supercritical carbon dioxide Brayton cycles: integration of cycle conceptual design and components preliminary design. *Applied Energy*. 276: 115354. https://doi.org/10.1016/j.apenergy.2020.115354

Zhu R., Zhang J., Zheng Q., and Zou J. (2008). Study of similarity problems concerning the working media helium and air in an axial-flow compressor. *Reneng Dongli Gongcheng/Journal of Engineering for Thermal Energy and Power*. 23 (6): 595–600.

Zou Z. and Ding C. (2018). A new similarity method for turbomachinery with different working media. *Applied Thermal Engineering*. 133: 170–178. https://doi.org/10.1016/j.applthermaleng.2018.01.034